CERN/DRDC 94-38
RD23/Status Report
6 October 1994

**Status Report on the RD-23 Project**

# Optoelectronic Analogue Signal Transfer for LHC Detectors

J. Feyt, E. Kling, W. Langhans, G. Stefanini * , F. Vasey
*CERN, Geneva, Switzerland*

J. Dowell, R.J. Homer, I. Kenyon, H. Shaylor, K.Webster, J. Wilson
*School of Physics and Space Research, University of Birmingham (UK)*

M. Glick, F. K. Reinhart
*Institute for Micro- and Optoelectronics- EPFL, Lausanne (CH)*

R. Cingolani
*MSDLE/University of Lecce and INFN Lecce (I)* §

P.G. Pelfer
*University of Florence and INFN Florence(I)* §

A. Bosacchi, S. Franchi
*MTI/MASPEC/Parma and INFN Milano (I)* §

P. Duthie, N.Green, A. Moseley, D. Robbins, D. Streames-Smith, N. Try
*GEC-Marconi (UK)*

K. Gill, G. Hall
*Imperial College, London (UK)*

G. Jarlskog, S. Kröll
*University of Lund (S)*

M. Holder
*University, of Siegen (D)* §

A. Baird, R. Halsall, S. Quinton
*Rutherford Appleton Laboratory, Didcot (UK)*

§ New participating Institute

Applications pending: CAEN (I), Europtics (UK), IRCS/Oxford (UK)

* Spokesman

## Table of Contents

## 1. Introduction

**The RD23 project was approved in February 1992. This second status report follows the first one [1] presented in September 1993. The aim of the project is to develop analogue optical links, based on electro-optic intensity modulators, for transferring signals from the front end electronics to the back end readout in LHC inner tracking detectors. The key issues are:**

- development of modulator arrays to be mounted on silicon and MSGC detector hybrid modules, with the following general requirements: very low power dissipation (a few mW), radiation hardness (dose D Å 10Mrad and fluence $\Phi$ (<$E_n$> Å 1MeV) Å $10^{14}$-$10^{15}$ n/cm$^2$ over Å 10 years), dynamic range Å 100:1, compact size.
- development of transceiver arrays (lasers, couplers, photodiodes), in hybrid or monolithic form, to be mounted on readout modules at the back end of the link.
- identification and test of rad-hard fibres and multi-way optical connectors.
- design of prototype readout modules for link performance evaluation.

The analogue links are mainly intended for the LHC tracker front-end designs based on analogue pipelines following the scheme outlined in Fig. 1.

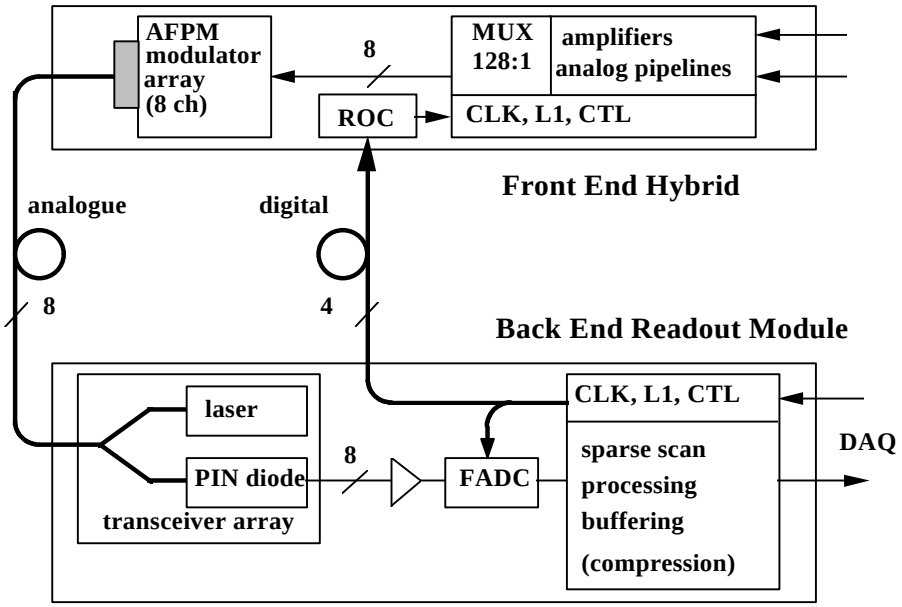


Fig. 1 - Functional blocks of optical readout architecture

The electro-optic modulators, mounted on the front-end detector hybrids, convert the pipeline sampled voltages into optical signals by modulating continuous-wave (CW) light from laser diodes coupled via optical fibres. The reflected modulated optical signals are converted back to electrical in transceivers on the readout modules at the back end. The transceivers are integrated devices and include lasers, couplers, photodiodes and possibly receiver amplifiers.

Digital optical links are used for transferring timing and trigger signals; these links may use some of the components developed for analogue transfer.

The work programme initially proposed by the RD23 collaboration included the investigation of electro-optic modulators in two technologies: a) Mach-Zehnder interferometric modulators (MZM) in lithium niobate (Ti:$LiNbO_3$), and b) asymmetric Fabry Perot electroabsorption modulators (AFPM) in III-V semiconductors. It should be pointed out that both modulator types are equally suitable for analogue and digital transmission.

The RD23 activity in the first year [1-3] was mainly aimed at investigating Mach-Zehnder modulators. A 16-channel MZM array was developed and tested. A detailed assessment proved that the MZMs can achieve very good linearity and large dynamic range, but also lead to major constraints. The polarisation maintaining fibres and connectors for the input port are expensive, and no fully satisfactory alternative scheme has been found to perform polarisation control in large systems at an affordable cost. The on-chip splitting leads to a relatively large device length that is difficult to fit in the detector hybrids. It would be possible to reduce the chip dimensions by scaling down to smaller splitting ratios, but this would also increase the cost per channel of the device.

It was concluded that MZMs on Ti:$LiNbO_3$ are not a cost effective solution for volume application in LHC experiments. However, the MZM array technique developed by RD23 has already found application in the NA-52 experiment, where a multi-channel device will be used to transfer the analogue signals from a set of Cherenkov counters at the target to the counting room over a distance of Å 350m with a bandwidth of DC to Å 300MHz [4].

In the course of the first year of activity, the collaboration was also able to carry out a preliminary investigation on the AFPM modulators. The AFPM are reflective devices, based on the electro-absorption properties of InGaAs/InP multi-quantum-well (MQW) structures on an InP substrate. A 4-channel array with micro-lens interface was fabricated and tested ([1], [2]). The preliminary results reported last year showed that the required linearity and dynamic range could be achieved with some additional effort.

The reflective link based on the AFPM requires only one input/output fibre. The AFPM are polarisation insensitive, and their vertical structure allows the fabrication of very compact arrays at affordable cost. The interface to optical fibres is much simpler than in waveguide devices. The advantages of the AFPM have been acknowledged and this technique has been retained for the continuation of the RD23 programme. The analogue readout based on AFPM is currently the baseline choice for the CMS tracker [5] and is being actively evaluated in ATLAS [6].

## 2. Overview of the main goals and results of past year activity

The following milestones were set in the past year programme:

- high priority studies of the new MQW devices;
- investigate the possibility of the construction of an advanced system demonstrator (integrated transceiver and laser), including production procedure and cost.

The main results of the RD23 activity are reported in this document. The development of MQW modulator arrays has been aimed at improving design, assembly and packaging. New devices with fibres butt-coupled to the modulator structures have been fabricated; preliminary tests results are reported in section 3. An investigation of several technologies suitable for developing an integrated transceiver has been initiated (section 4). A prototype readout module has been developed, using discrete fibre optic components, to be used as a general purpose tool for link evaluation and as an evolving platform for testing more advanced designs (section 5). The overall link performance has been assessed in lab measurements and preliminary results have been obtained in beam tests with Si microstrip detectors. Substantial progress has been made in assessing the capabilities of the technique and in the overall system design (section 6). The effects of γ-ray irradiation on modulators and single-mode optical fibres have been investigated (section 7).

New participants have joined the collaboration and other applications are under way; the proposed work programme, sharing of responsibilities and budget for next year activity are discussed in section 8.

## 3. Reflective AFPM modulators

The characteristics of the reflective AFPM modulators have been investigated on pigtailed arrays fabricated by GEC-Marconi Materials Technology (GMMT). The semiconductor structures are all based on an existing mask configured as a linear array of 8 channels, with active MQW areas of 30μm diameter on 125 μm pitch. Since the pitch of

the fibres in a ribbon is 250μm, every other MQW element is actually used, so that each packaged device contains 4 pigtailed channels.

The first prototypes used a trial assembly technique in which the single-mode fibre ribbon was interfaced to the modulators through the transparent substrate using relay microlenses.

Preliminary results with these devices were presented in our previous status report and a more detailed evaluation is reported here (section 3.1).

Two major improvements have been implemented (section 3.2):

- a novel assembly technique has been developed, in which the fibres are butt-coupled to the modulators through the thinned substrate. This provides improved thermal stability, lower losses and cost-effective assembly suitable for volume production;

- flat polished MT connector ferrules have been replaced by angle polished MTs with higher return loss (> 50dB); this results in a substantial reduction in the interferometric noise in the link, without the need for index matching gel. The angle-polished MT ferrules have recently become commercially available; they are now installed on all new modulator arrays and are being retrofitted on the trial units.

### *3.1 AFPM with micro-lens interface*

In this section we summarise the results of the measurements on 14 working channels out of 4 packaged arrays. Two of these arrays (#4 and #5) were pigtailed with conventional flat polished MT ferrules. The other two (#7 and #8) were improved devices equipped with angle polished MTs. The typical transfer function of an AFPM (ch. 3 of assembly #4) is shown in Fig. 2.

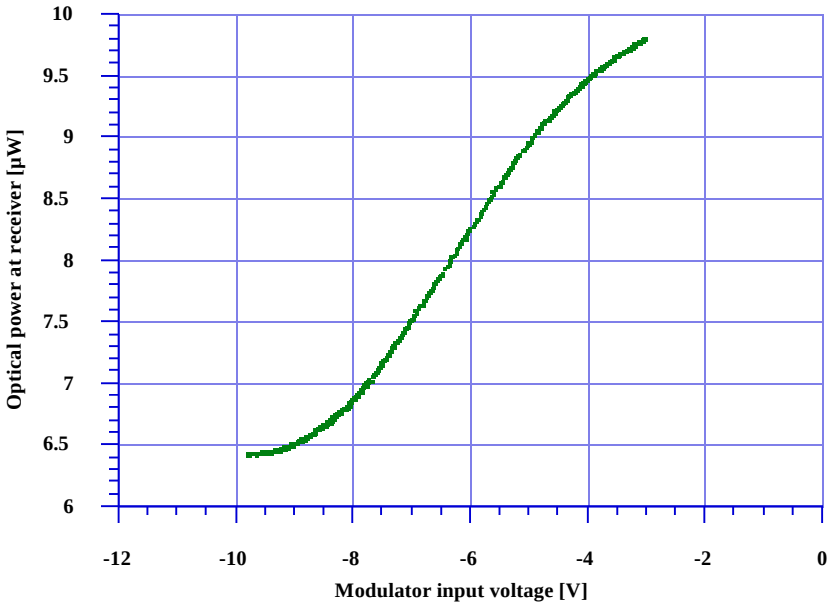


Fig. 2 - AFPM transfer function

The laser power launched in the modulator pigtail is Å 65 µW @ 1538nm. The central region of the transfer function shows linear response (Fig. 3), with an integral non-linearity contained within Å 2% of full scale for input signals in the range of ±1.5V relative to the half-point bias. The full linear input range corresponds to a reflectance change δR Å 10%.

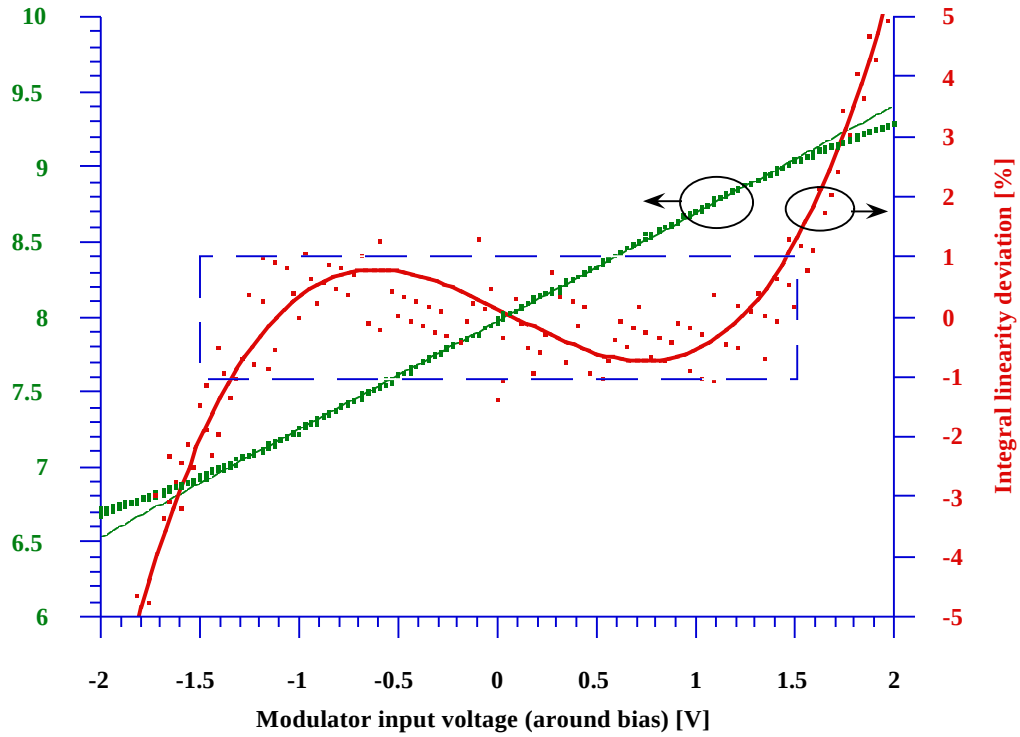


Fig. 3 - AFPM linearity response

The modulation response and signal/noise ratio (S/N) in the different AFPMs have been compared using a new receiver (section 5) with very low equivalent noise input ($I_n$ Å 2.5pA/ÃHz). Measurements were taken with an input sine wave of amplitude δV = 1Vpp (corresponding to Å 35% of the available dynamic range) and a CW laser power $P_i$ Å 75µW launched in the fibre.

The response of different channels is shown in Fig. 4. The spread can be accounted for by small differences in the assembly process. The peak-signal to rms noise ratio was S/N Å 25 (typ.) in a bandwidth BW Å 30MHz. The achievable S/N for full range modulation is discussed in section 6.1.

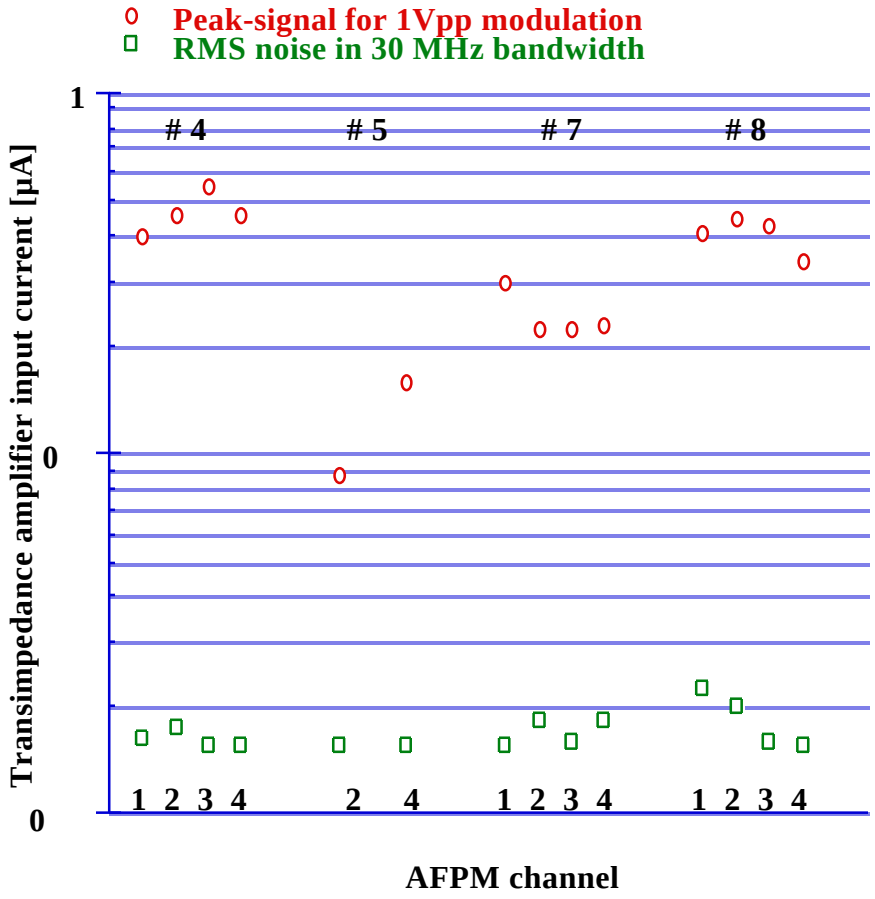


Fig. 4 - Comparison of modulator channels (micro-lens coupled devices)

### *3.2 AFPM with butt-coupled fibres*

We have recently developed a novel assembly in which the fibres are butt-coupled to the modulator active areas through the modulator substrate, which is thinned down to Å 100µm for this purpose. The assembly technique is based on a precision drilled spacer which determines the position and the orientation of the fibre ends with great accuracy. The semiconductor chip is positioned on the spacer by flip-chip bonding. A thin (Å few µm) layer of optical glue assures the optical contact between the fibres and the semiconductor chip. The packaged array (Fig. 5) has a footprint of Å 10x10mm and a height of Å 6mm.

The prototypes are provided with "gull wing" leads, for simplicity of fabrication; production devices will have solder pads or possibly be made as plug-in units to ease

detector test and mounting. The fibre ribbon pigtail has a length of several meters with a multi-way connector at the end, to provide a convenient breakout immediately outside the tracking detector region for installation in the experiment.

Two trial devices have been made available for evaluation very recently. The results reported here are still preliminary and will have to be confirmed by further measurements on the batch of units in preparation.

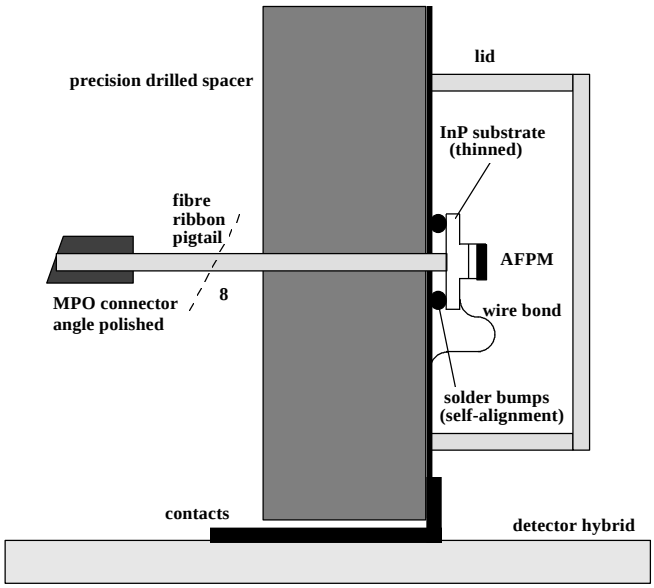


Fig. 5 - Schematic of butt-coupled AFPM

The butt-coupled AFPMs include an improved design of the Fabry Perot cavity. On-wafer tests have confirmed that the tuning of the FP cavity resonance and the movement of the excitonic edge have fully met the design objectives. However, an as yet unexplained (at the time of writing) broadband loss has resulted in a lower than expected overall reflectance and modulation efficiency. This is confirmed by the preliminary results (Fig. 6) obtained in the same test conditions as in section 3.1.

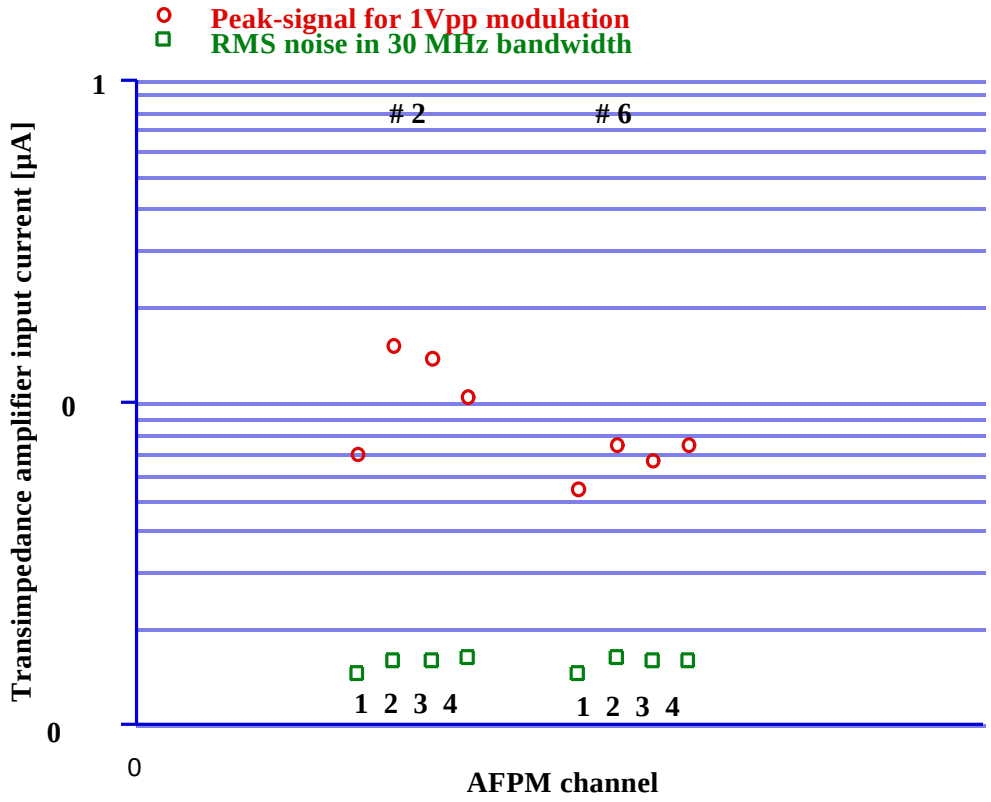


Fig. 6 - Comparison of AFPM channels (butt-coupled devices)

The largest S/N ratio is lower by a factor Å 3 with respect to the previous microlens-coupled devices. The manufacturer is currently investigating the causes of the reduced reflectance.

The optical insertion loss in the butt-coupled devices is equivalent to that of the microlensed devices, but is achieved in a compact package that is compatible with detector requirements. Other advantages of the new assembly are the much lower sensitivity to temperature changes (tested so far in the range ΔT Å 20 _C to 30 _C) and considerably reduced interferometric noise.

### *3.3 Effects of magnetic field and temperature changes*

General theoretical considerations indicate that the response of the AFPM modulators should be rather insensitive to magnetic fields such as those found at LHC. This has been

confirmed by direct measurements on several MQW samples of varying well width (5 nm to 11.5 nm).

At Birmingham, the samples were placed in a warm bore superconducting solenoid that allowed fields up to 12 T in the direction parallel to the MQW growth axis (the field orientation for which the largest effect would be expected). The transmission spectra were measured at room temperature; from these measurements, the shift in energy (wavelength) of the exciton peak and the change in peak absorption coefficient could be obtained. At the MSDLE/Lecce, similar measurements were performed at cryogenic temperature ( Å 4K) and fields up to 8 T in a dedicated magneto-optic spectroscopy facility, where the relative orientation of the field and the sample could be varied. The exciton peak shift with magnetic field should not depend on temperature; the measurements at both sites for the same field orientation indeed show good agreement [7].

Fig. 7 - Model predictions for ΔR vs B (field parallel to the MQW growth axis)

The exciton peak shift is described by $\Delta E = c_1(w)\, B^2 + c_2(w)\, B^4$ where w is the well width. The parameters from the fit to the measured data have been included in the device model, from which the induced reflectivity change δR is derived. It is found that in the worst case (field parallel to the growth axis of the wells) the induced δR is relatively small (δR <2% at B=4T with bias voltage $V_b$ Å -7 to -10 V) and varies only slightly with well width (Fig. 7). The effect of fields normal to the growth axis is considerably smaller.

We conclude that the magnetic fields of the LHC detectors are not expected to induce any significant degradation in the link performance. Direct measurements on pigtailed modulators will be performed on the new devices which have suitable non-magnetic cases.

The main effect of temperature fluctuations is to change the relative positions of the excitons and the cavity wavelengths. According to the device model, the dependence of the reflectivity on temperature changes relative to the design value is asymmetric: ΔR Å -0.25% for ΔT = +10 _C and ΔR Å -2.5% for ΔT = -10 _C. Since the effect is non-linear, these model predictions should not be extrapolated to larger temperature changes. They show however that the modulator operating temperature range for best performance will cover approximately the range +15 /-5 _C around the design value, which can be tuned to the detector requirements. Outside this range the performance will start to degrade but will still be adequate for monitoring purposes. We have not been able yet to confirm the model predictions on the microlensed devices where the thermal effects due to the assembly (glued elements) predominate. Measurements are under way on the new butt-coupled devices.

## 4. Integrated transceivers

Each channel of the reflective link (Fig. 1) requires a transceiver (laser/coupler/photodiode). In the present demonstrators, where a single laser feeds all channels in a modulator array, fused splitters and couplers are used. Discrete fibre optic components are commercially available, and offer a satisfactory solution in systems with a small number of channels. The volume production of transceiver for the LHC application requires cost-effective solutions. A preliminary comparison of the main alternatives can be summarised as follows:

- integrated optics on glass. Passive optics (splitters and couplers) are implemented in planar technology (optical waveguides on a planar glass substrate). Lasers and photodiodes are connected by fibres. This technology is well suited for volume production. However, inquiries with several vendors prove that this solution would be too expensive;

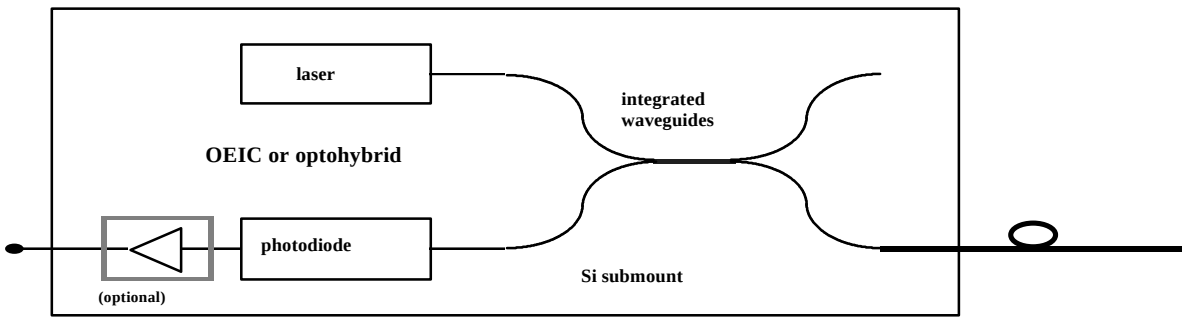

Fig. 8 - Schematic of integrated transceiver

- monolithic opto-electronic integrated circuits (OEIC) on silicon submounts (Fig. 8). This technology has been demonstrated on several components. A key issue in the reflective link is to reduce the optical loss in the coupling of the silica fibre interface to the InP substrate waveguide. This might be achieved using tapered low NA waveguides, but substantial development work would be required. The OEIC offers potentially the lowest production cost if a satisfactory yield can be achieved;
- planar opto-hybrid (Fig. 8). Silica-on-silicon waveguides allow for high efficiency coupling to optical fibres, aligned by using V-grooves. Lasers and photodiodes are die components. This technology may not lead to the lowest volume production cost, but the development would be less expensive and can be accomplished more rapidly than in the case of an OEIC. We expect that a prototype can be delivered by Å end 1995.

A detailed investigation of the different technologies is under way. The development of the integrated transceiver is a key issue and a milestone of the RD23 programme for next year.

## 5. Readout module

During the tests of the trial prototypes it was felt that a flexible and modular receiver board would be required for more advanced work. For this purpose, the CERN team has developed a module that is mainly a general link evaluation tool but is also the platform for a more complex system; the block diagram is shown in Fig. 9.

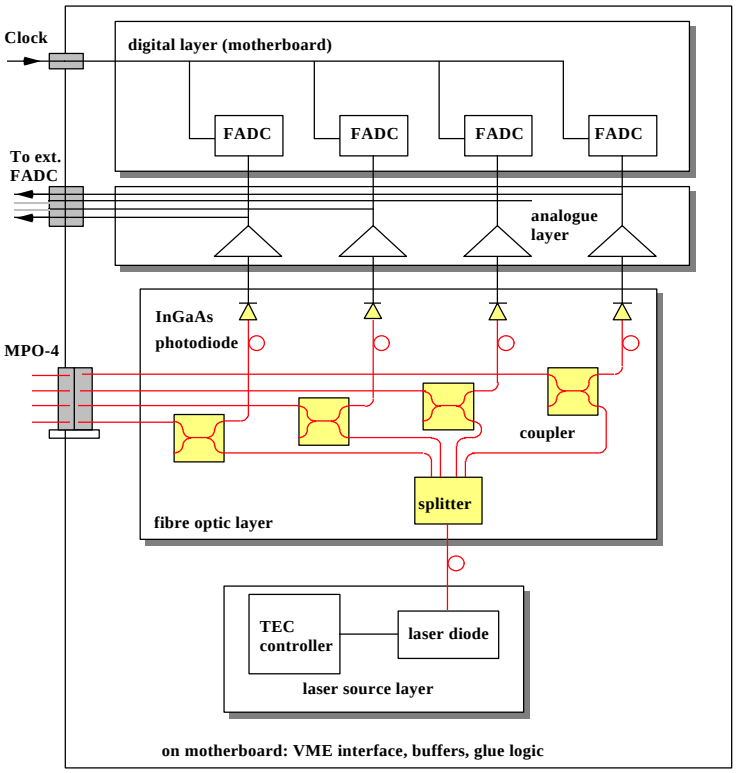


Fig. 9 - Schematic of readout module prototype

(4 channels only shown)

The 6U VME module is designed to contain 8 channels: splitter, couplers, receivers (InGaAs PIN photodiodes, amplifiers), 8-bit FADCs and FIFO buffers. Low noise transimpedance amplifiers ($I_n$ Å 2.5pA/ÃHz), followed by a 50X differential gain stage, assure an overall equivalent differential transresistance $R_T$ Å 700kOhm, with a bandwidth BW > 40MHz. The amplifiers, mounted on daughterboards, deliver signals (< 2Vpp amplitude for full linear modulation range) to the internal FADCs as well as to external digitizers through front panel connectors.

The optical couplers - discrete fused fibre components - are assembled on a separate layer and fusion spliced to the photodiode pigtails. The laser diode feeds the modulator channels via an optical splitter. Data are accessed through the VME interface and are also available on a parallel bus for fast transfer to auxiliary processing modules. A prototype with 4 operational channels has been assembled and has been used for the measurements reported in this document. The design of the unit is not aimed at high packing density but rather at full modularity so that the different sections can be easily serviced and replaced by improved versions as they become available. This allows evaluating different amplifier configurations and laser diodes. The module is an efficient tool for lab and beam tests and is presently requested by several groups. Negotiations are currently under way with industrial firms in view of engineering the module for small-scale production.

In parallel with this development, RAL has undertaken, in the framework of the ATLAS and CMS experiments, a general top-down design study of a large size single-width VME-

type board with up to 64 optical channels [8]. Integrated transceivers are required to achieve this high packing density. The board will have full capabilities, including clock deskewing and distribution, data reduction and addressing, fast interface to the DAQ system. Prototypes with full signal processing functionality (but without integrated transceivers) are expected by mid '95.

## 6. Link performance

Once packaged, the AFPMs can only be evaluated within a complete optical link, including a transceiver and a fibre ribbon patchchord. The overall link performance is then determined by the contributions of the individual elements. In particular, all interfaces (changes of propagation media) in the light path are traversed twice by the forward and backward propagating beams and have critical impact on signal and noise characteristics. The results reported hereafter were obtained using the fused fibre transceiver included in the readout module prototype (input transimpedance stage with $I_n$ Å 2.5pA/ÃHz) with a Å 100m long fibre ribbon and in a bandwidth BW Å DC to 30MHz. The modulator under test was unit #8 (microlensed device) fitted with an angle polished MT ferrule.

### *6.1 Signal to noise ratio*

The S/N ratio that can be achieved with the full-scale linear input modulation is determined by the contributions of the various noise sources: laser relative intensity noise (RIN), equivalent input noise current $I_n$ of the receiver amplifier, shot noise, and interferometric noise. We have evaluated the link performance with two types of laser diodes:

- a Fabry Perot multimode laser, which is not very sensitive to back reflections and therefore allows a robust operation of the link. However, the relatively high laser noise (RIN Å -135dB/Hz) sets a limit in the S/N ratio;

- a distributed feedback (DFB) laser, which features extremely low RIN (< -150dB/Hz) but is very sensitive to back reflections so that intensity noise may be generated, even when angle-polished ferrules are used. To avoid this, an optical isolator is usually required, together with high-frequency (Å 200MHz) laser line dithering by RF modulation.

The maximum peak-signal to rms noise ratio S/N has been measured with a laser power $P_i$ Å 0.20mW launched into the modulator pigtail at full-scale linear range modulation input of $\delta V$ = 3Vpp. We have obtained S/N Å 90 with the FP laser diode, and S/N Å 130

(typ.) in the case of the DFB laser diode, when the interferometric noise is reduced to a minimum. The results are plotted in Fig. 10.

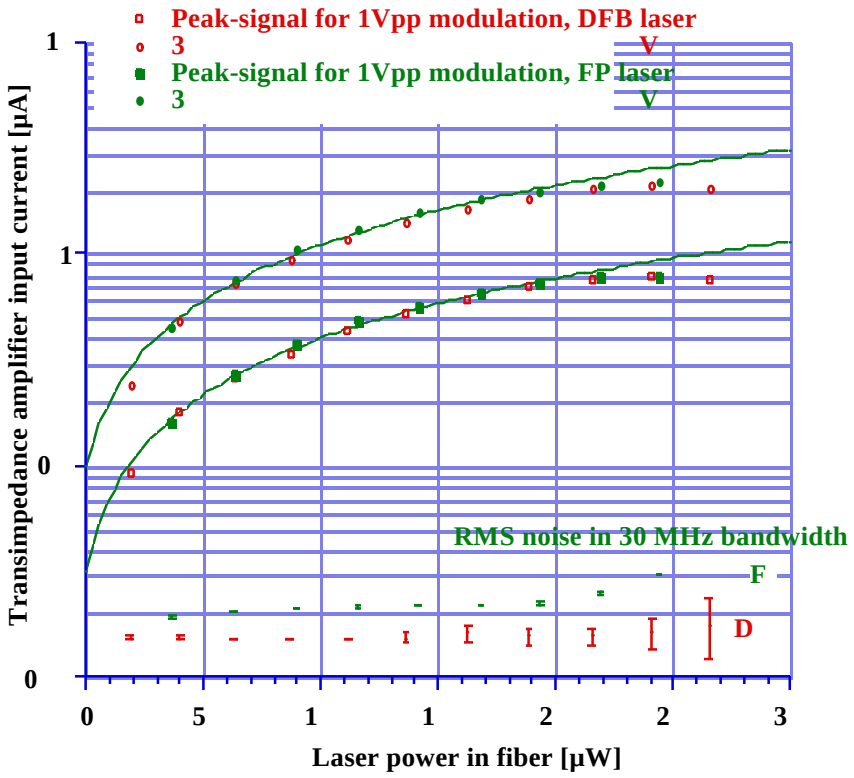


Fig. 10 - Peak-signal to rms noise ratio in the microlens coupled AFPM

We would expect the S/N ratio to increase with laser input power up to a limiting value (S/N> 200) determined by the laser RIN. We find, however, that when the laser power is increased above Å 0.2mW, the noise level also increases above the level expected from shot noise and RIN contributions, and it appears that S/N Å 150 is the best result that can be achieved at present. The effect is not yet entirely understood but is probably due to additional laser and/or interferometric noise resulting from the higher optical power. Tests are under way to clarify this point.

Several improvements are envisaged to increase the S/N ratio. Firstly, a (slight) reduction in the noise floor at low optical power can be obtained by using a lower noise transimpedance input stage; devices with $I_n$ Å 1.8pA/ÃHz are commercially available and will be used in future versions.

Secondly, the maximum reflectivity change can be increased by improving the wafer growth and processing. The industrial partner is confident that ΔR Å 0.25 to 0.3 will be obtained with optimised parameters in the next run. This will increase the S/N ratio by Å 30% relative to the best results obtained so far.

Thirdly, a further enhancement can be achieved by stacking two MQW regions; the stacked MQWs would be driven electrically in parallel, but the light would pass through both, so that the overall modulation depth would be doubled. These subjects are being investigated in parallel with the evaluation of the new butt-coupled devices.

### *6.2 Lab and beam tests with Si microstrip front-end electronics*

The overall performance of the link was evaluated in lab tests by comparing its response to a copper link. The input signal was a pattern of voltage steps generated by a Lecroy 9109 Arbitrary Function Generator, injected simultaneously into an RG-58 coaxial cable and into an optical link (length Å 100m). The output signals were measured with a digital scope (8 bit resolution) and the data were collected and analysed using a LabVIEW-based DAQ. The two waveforms were normalised and the relative delay was determined by cross-correlation. Samples corresponding to the same region of the waveforms were compared and the error signal was evaluated. We found an approximately Gaussian distribution of the measured differences, with a deviation $\sigma$ Å $\sigma_n$, where $\sigma_n$ is the overall receiver noise contribution.

The performance of the optical link has also been evaluated in beam tests of Si microstrip detectors connected to the APV3 front-end chip (Fig. 11).

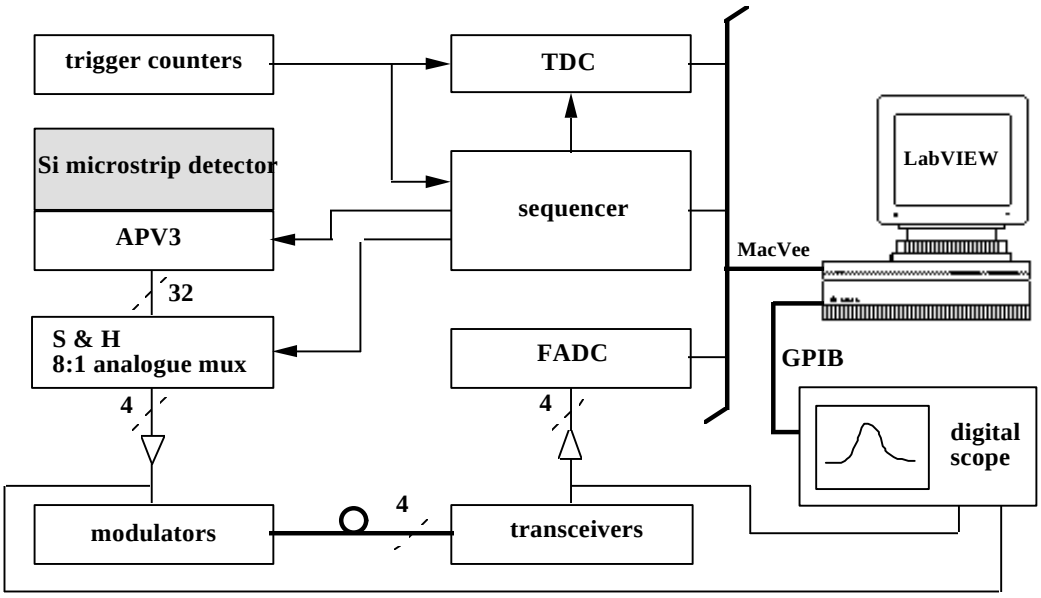

Fig. 11 - Schematic of beam test setup

The chip contains 32 channels and includes analogue pipelines and APSP processors. The Si detectors, sequencer and DAQ were provided by Imperial College. For the purpose of the link tests, the sampled voltages from the 32 channels were multiplexed in groups of 8 into 4 optical links, using an external analogue multiplexer running at Å 10MHz.

The peak-signal amplitude was adjusted to either 0.4 or 0.8V for ~2MIP energy loss, corresponding to a uni- or bipolar operation of the modulator. The remaining portion of the available link linear range (up to 3V) was reserved to allow for the different and varying pedestal levels generated by the APV3 chip. The link was operated continuously for 36 hours with no degradation of the signal or noise characteristics. The only minor adjustments needed were due to the effects of temperature fluctuations in the beam area (a few degrees _C) on the micro-lens coupled assembly.

Beam data were acquired successfuly both with copper and fiber links; the analysis of the measurements is currently under way.

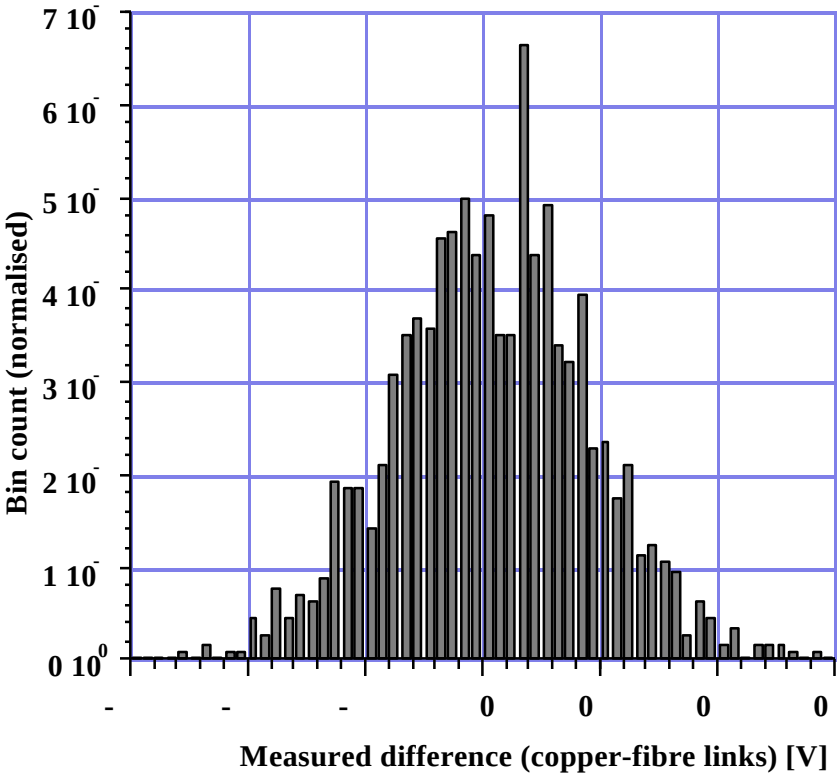

Fig. 12 - Comparison of optical and copper links

Fig. 12 shows the distribution (over 160 events) of the measured deviation of the signals from channel 3 measured simultaneously with both links. We find a standard deviation of σÅ8.4mV (rms) for a mean 2 MIPs signal amplitude $V_S$ Å 170mV (signal-peak Å0.8V at modulator input, laser power Å200µW in fibre).

### *6.3 System aspects*

While the milestones of our project are mainly determined by technical advances in modulators and integrated transceivers, we have become increasingly aware of system aspects that are equally relevant for the feasibility and performance of the optical link. Some of the key issues that are being investigated are reviewed in this section.

Modulators are being developed as 8-channel arrays to make best use of the modularity of fibre ribbons and connectors that are industry standard. This modularity fits well a large part of the inner tracker detector elements and front-end electronics, with the devices mounted directly on the detector hybrids. In certain cases, it may be more cost-effective to mount the modulators on separate boards and fan-in the signals from two or more detector elements. The requirements on electrical line drivers and connectors are being investigated in collaboration with LHC experiments.

Digital optical links are required for distribution of the timing, trigger and control signals from the readout crate to the front-end electronics. In the scheme presently considered, the digital link would share a common ribbon with the analogue readout fibres.

To minimise cost and material budget, it would appear attractive to integrate 4 photodiodes together with 8 modulators in the same package, which will then be pigtailed with a 12 fibres ribbon. However, cross-talk (to be assessed) might prevent this integration. In this case, the 12 fibre ribbon will be bifurcated into an 8-way ribbon terminated in the modulator package and a 4-way ribbon terminated in the photodiode package. This latter approach allows optimising separately the two chips and possibly integrating the photodiode amplifier within the package. Similarly, at the readout end, the 12 fibre ribbon will be bifurcated and terminated on an MT-8 and an MT-4 ferrule, for analogue and digital respectively. This technique would be cost-effective and allow for possible redundancy.

The digital transmitters could be integrated low-power laser arrays, used in pulsed mode. The unavoidable differences in the lengths of the fibres carrying the timing signals will be compensated for by the deskewing circuitry in the readout module.

The fully analogue readout of a 12M channels inner tracker may require up to Å 100k fibres. The deployment of such a large number of fibres in the detector is a challenging task and requires enhanced packaging and connectivity. A general scheme for the optical cabling has been developed (Fig. 13).

We propose to use high-density matrix connectors (HDMX), developed and manufactured by Europtics, which make use of the MT ferrule and provide more than 100 optical connections in approximately the size of a DIN 41612 connector shell.

Fig. 13 - Schematic of fibre cabling for the analogue optical readout

The matrix connectors contain MT ferrules which conform to CECC (the HDMX itself is being submitted both to the IEC and the CECC for standardisation). The matrix connectors will be mounted on the bulkheads of the fibre cables, which will be installed pre-terminated, as well as on dedicated optical backplanes in the crates of the readout system. This approach allows the fibre optic cables to be assembled and tested at the factory, and provides breakout points that make installation easier.

A detailed budgetary cost estimate based on this scheme has been done and will be included in the ATLAS and CMS Technical Proposal.

## 7. Irradiation of modulators and fibres

### *7.1 Modulators*

Modulator structures had been irradiated with neutrons, as reported in our '93 report, at the ISIS facility at RAL with fluence $\Phi$ ($<E_n>$ =1MeV) Å 1.3 $10^{14}$ n/cm$^2$ . The induced (optical) change in spectral reflectance modulation had been found to be very small and barely observable with the most sensitive instrumentation. The leakage current of the MQW devices had increased, in some cases, from Å 5nA to Å 100nA; this change, of no practical consequence, had been attributed to surface effects.

Modulator structures have recently been irradiated at the Imperial College $^{60}$Co gamma source, together with optical fibres; the experimental setup is shown in Fig. A1.1 in appendix A1. The accumulated dose was D Å 20Mrad, with a dose rate dD/dT Å 205krad/hr. Reflectance spectra were measured before and after irradiation, while the leakage current was monitored throughout the irradiation and recovery periods.

We found that gamma irradiation does not induce any measurable change in reflectance modulation.

Leakage current (at voltage bias Å -7V) increased to a saturation level of Å 100nA in some MQW devices, while it was not affected in others (Fig. 14).

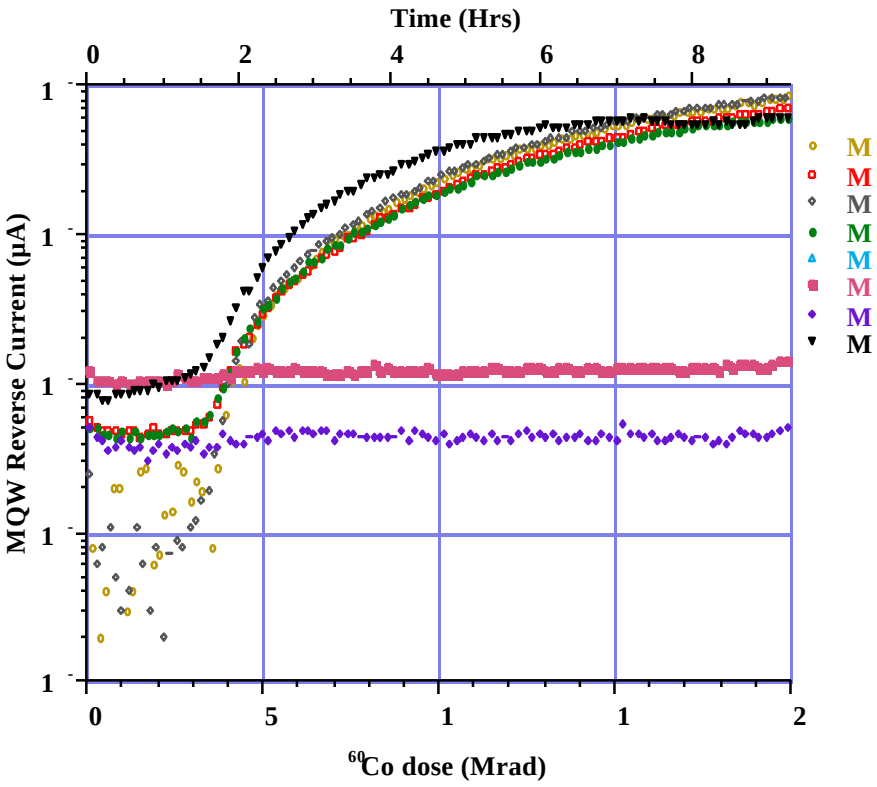


Fig. 14 - AFPM samples - Leakage current under gamma irradiation

Full recovery was observed in all cases, as shown in Fig. 15.

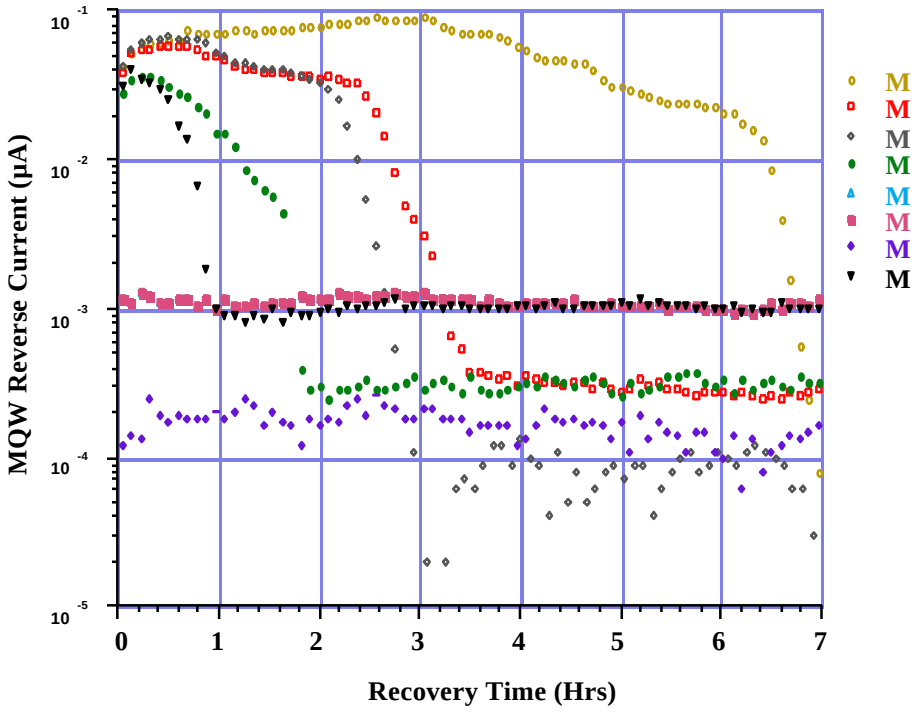


Fig. 15 - AFPM samples - Leakage current recovery

The increase in leakage current is attributed to the presence of a polyimide layer in the device structure; bulk InGaAs PIN diodes without this layer had been previously exposed to higher doses with no adverse effect.

The results obtained so far indicate that the MQW structures are capable of withstanding the most severe radiation constraints at LHC without any significant degradation in optical and electrical performance. We plan to extend the irradiation measurements to the new butt-coupled devices, including the in situ monitoring of the optical properties during exposure.

### *7.2 Fibres*

The attenuation characteristics induced by neutron and γ-ray irradiation on optical fibres has been extensively investigated in several laboratories, particularly in view of the applications at nuclear power plants. Since the induced loss is considered to be related to the defects or "colour centres" introduced by dopants such as Ge, pure-silica core fibres are

expected to suffer the lowest loss. Theoretical models and experimental results can be found for example in [9].

We have measured the neutron and γ-ray irradiation effects on several fibres, mainly single-mode (SM) types. All the fibres under test are commercially available products. This section contains a summary of the main results; more details are given in appendix A1, and a full report will be submitted for publication [10].

Neutron irradiation runs were performed in 1993 at the SARA facility in Grenoble. This facility delivers neutrons with a mean energy of 6.2MeV from the Be(d,n)B reaction for irradiation at room and cryogenic temperature with fluence $\Phi$ Å $5x10^{14}$ n/cm$^2$. It may be recalled that $\Phi(<E_n>=6.2MeV)$ Å 0.7 $\Phi(<E_n>=1MeV)$ for the same nonionising energy loss. The photon contamination is relatively low (Å 22% of the total dose in $CH_2$ materials).

The samples irradiated at SARA included standard telecom SM Ge-doped and SM pure silica core, fluorine doped (PSC/$F_2$) fibres. Sample length was Å 70m. The typical induced attenuation (@ $\lambda$ = 1.3μm and T Å 20 _C) for a neutron fluence $\Phi$ Å $10^{14}$ n/cm$^2$ is shown in the following table:

Table 7.I - Main results of neutron irradiation at the SARA facility

| SM Fibre type | $\Phi(<E_n>$ Å 6.2MeV) (n/cm$^2$) | Induced loss (dB/100m) |
|---|---|---|
| PSC/$F_2$ | $1.2x10^{14}$ | 0.25 |
| Ge doped | $4x10^{13}$ | 1 |

These results were obtained at a fluence rate of Å $3.6x10^{12}$ n/cm$^2$.hr, while the corresponding rate at LHC, assuming 6 months/year operation, would be Å $5x10^{10}$ n/cm$^2$.hr. In those conditions, taking into account the fibre recovery, the overall neutron induced loss will be considerably smaller and it can be expected to have no significant effect on the link performance.

In the case of γ-ray irradiation, it is well known that dose rate effects can be very significant. The measurement of induced loss in a laboratory environment generally requires very high dose rates in order to reach a given accumulated dose D during irradiation runs that usually do not exceed a few days, for practical reasons. Detailed models have been developed to extrapolate results in the case in which the same

accumulated dose D is reached in a period of many years. This is the case in the inner tracker region at the LHC, where a total dose D Å 10Mrad is accumulated over 10 years with a dose rate of a few hundred rad/hr .

We have irradiated three types of single-mode fibres at the Imperial College $^{60}Co$ gamma source:

- pure silica core, fluorine doped cladding ($PSC/F_2$) - same as in the neutron irradiation tests (types 1 and 2);
- match clad (MC), Ge-doped core for telecom applications (type 3).

We find that the induced loss is determined mainly by two terms: one depends only on the *total dose*, while the other is *dose rate dependent* and tends to saturation with increasing total dose. The dose rate dependent term is conveniently represented by the sum of two (or more) exponential components with different relaxation times. The dose rate dependent terms would give negligible contributions at the low dose rates found in the tracking region at the LHC. The detailed model (appendix A1) predicts that the induced attenuation over one year due to the linear term, in the worst case in which it would not recover during the shutdown period, would be smaller than Å 0.6dB/100m.

In our scheme, the use of rad-hard fibre would be limited to the modulator pigtail which is most exposed to high radiation levels. The pigtail is terminated into a connector to assure a convenient breakout during the assembly. We assume that in the worst case the length of the pigtail would be Å 10m, which would lead to an overall induced attenuation of less than 0.6dB after 10 years of LHC operation. It is interesting to note that, in the case of very low dose rates, the induced loss in the MC fibre, a Ge-doped type, seems to be comparable and even smaller than in the $PSC/F_2$ fibres. However this type of fibre would be very sensitive to increased background levels or even minor beam spill accidents (dose rate), and we expect that it would show poor performance under neutron irradiation.

These results show that the radiation induced loss in the most exposed section of fibres - the modulator pigtail in the central region of the detector - will be negligible through the lifetime of an LHC experiment if single-mode $PSC/F_2$ fibres are used in the 1.5µm wavelength window. These fibres are commercially available from several vendors at a slightly higher cost than standard telecom SM Ge-doped fibres, which can be safely used in the outer layers and for cabling in the experimental hall.

## 8. Participants, programme and budget for next year

### *8.1 New participants*

The University of Siegen and a consortium of Italian institutes, including participants in ATLAS, have recently joined the collaboration. The Italian consortium also includes researchers from the Department of Materials Science of the University of Lecce (DMSLE) and from the MTI-MASPEC Institute at Parma (a national facility for information technology and III-V semiconductor compounds developments), with funding assured by national agencies.

The Interdisciplinary Research Centre for Semiconductor Materials (IRCS) in Oxford (Prof. G. Parry and M. Whitehead) is also joining the collaboration with a specific programme of low temperature studies of optical modulators (for LAr detectors). This programme is in collaboration with industry (GEC-Marconi Materials Technology) and independently funded.

On the industry side, Europtics (UK) and CAEN (I) have expressed their interest towards joining RD23. Europtics has actually been involved in our programme since the start through our present industrial partner, and provides expertise in optical connectors and fibres. CAEN would contribute to readout electronics developments. We expect that both applications will be effective very soon.

Other experiments, in Europe and elsewhere, have established contacts in view of adopting the modulator technique, for digital as well as for analogue transmission. In particular, the analogue readout based on AFPM is being considered for the NESTOR deep water neutrino telescope. It is worth pointing out that in this case the length of the fibre is Å 20km; lab measurements at CERN have shown that satisfactory link performance can still be achieved.

### *8.2 Work programme*

We propose a work programme with the following milestones:

- Complete the development of the modulator array in butt-coupled design. This involves the following three major issues. Firstly, to produce a new mask with 8 active channels placed at the required pitch of 250µm. Secondly, to produce a small batch of devices with increased maximum reflectivity change. Thirdly, to investigate the direct butt-coupling of fibres to the active modulator structures, which would

result in a significant reduction in insertion loss. For this purpose a redesign study of the mirrors structures is required.

- Develop an integrated transceiver. This requires further investigation of the key technology issues, including the laser configuration for low RIN and insensitivity to back reflections. A prototype array will be assembled and packaged.
- Continue the investigation on the effects of neutron and γ-ray irradiation of modulator arrays, fibres and connectors.

The following key issues will also be considered:

- Improve the design of the readout module and evaluate the overall performance using discrete fibre optic components and laser diodes.
- Pursue the evaluation of the full link with butt-coupled modulators, including fibre ribbons and multiway connectors, in beam tests with silicon and micro-strip gas chamber (MSGC) detectors. Assess the most suitable technique for integrating the modulator array onto the detector hybrid.
- Investigate the techniques for implementing the digital optical link that will transfer the timing, trigger and control signals from the readout back end to the front end electronics. The digital link may use components developed in the present programme.

The sharing of responsibilities will be very similar to the one in the previous year. Beam tests with detector modules are scheduled in CMS and ATLAS; the Imperial College and Birmingham teams, respectively, will assure the interface to the experiments. Additional support and resources will be provided by the institutes which have recently joined RD23 and by the new partners as soon as their participation will be confirmed.

### *8.3 Budget*

The proposed budget is shown in the following table:

The proposed budget includes funding for the milestones in the work programme. A major share of the budget will be dedicated to the development of the integrated transceiver prototype.

The contribution of our industrial partner will correspond to 50% of the development cost of the optoelectronic devices, as in the previous years.

On the basis of past experience, we assume that CERN will have to support the main contribution to funding the device developments. This will certainly change when the major share of the cost will be in providing pre-production quantities of links for extensive tests in LHC experiments. We are confident that this will be the case at the completion of the proposed work programme for year 3. We also hope that the institutes that joined recently the collaboration will be able to assure a significant contribution to the funding of the project.

| Activity | kSFr | CERN |
|---|---|---|
| Transceivers (& modulators) development | 710 | 190 |
| Electronics | 60 | 30 |
| Radiation tests | 50 | 10 |

**Appendix A1 - Gamma-ray irradiation of optical fibres**

Samples of the fibres (spools of Å 90m length) were irradiated at the Imperial College $^{60}Co$ gamma source. The experimental set up is shown in Fig A1-1. A pigtailed laser diode was used to launch Å0.35mW CW optical power at λ Å 1.55µm into the fibres via a 4-way splitter. The optical power launched into the three fibres under test was in the range of 50 to 100µW. The fourth fibre was not irradiated and was used to monitor fluctuations in the laser output.

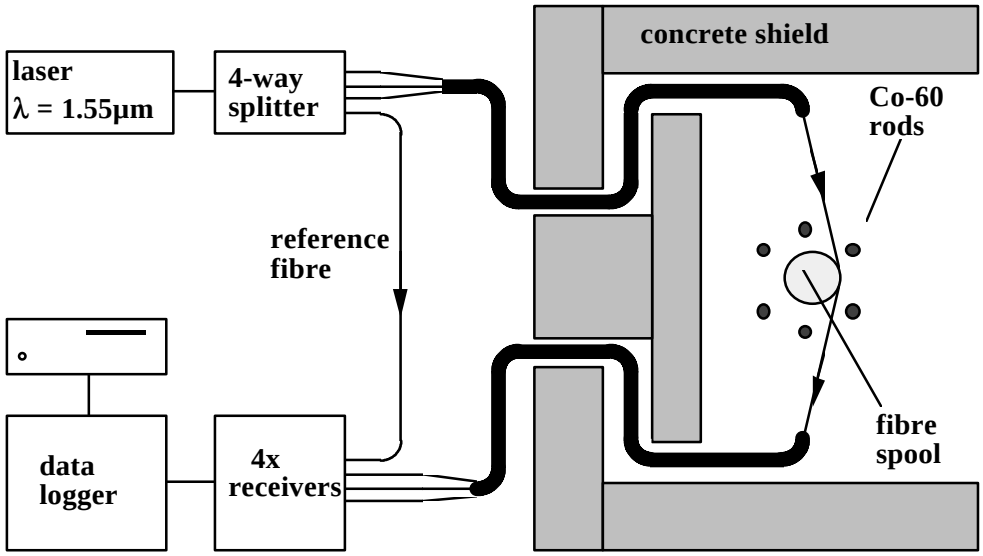


Fig. A1-1 - Experimental setup for irradiation of fibres with $^{60}Co$ γ-ray source

Measurements were taken at 60s intervals over six days during the irradiation, and for a further 32 hours after the irradiation in order to collect data on recovery. The accumulated dose and the dose rate were accurately measured for each fibre and are shown in table A1-I:

Table A1-I - Total dose and dose rates

| SM Fibre type | Dose D (Mrad) | Dose rate (krad/hr) |
|---|---|---|
| $PSC/F_2$ (type 1) | 36 | 268 |
| $PSC/F_2$ (type 2) | 24 | 175 |
| Ge doped | 29 | 211 |

The time profile of the induced loss and recovery is shown in Fig. A1-2 for the three fibres.

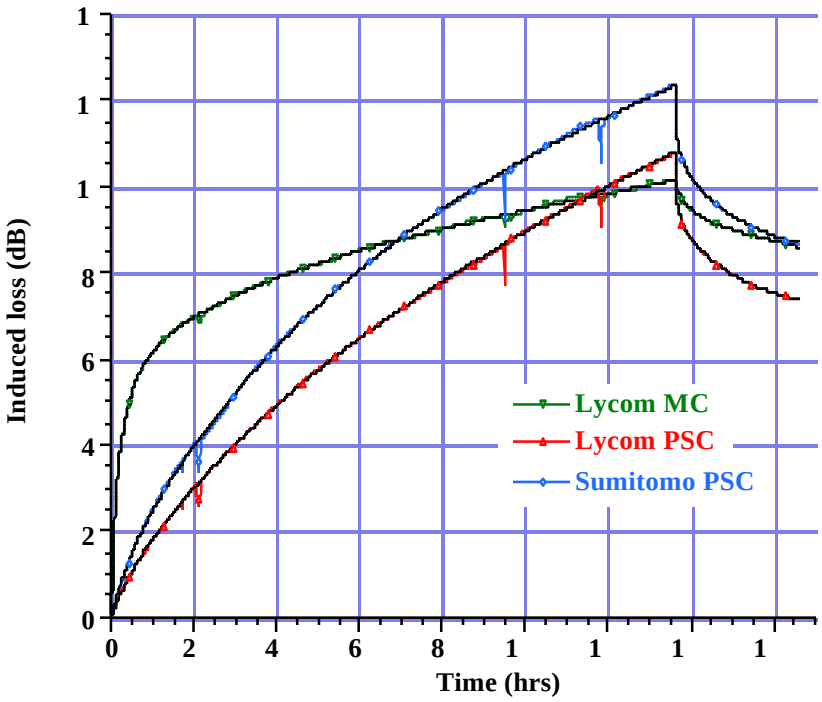


Fig. A1-2 - Time profile of induced loss and recovery (fibre length Å 90m)

The data were fitted using the kinetic model referred to in [9], which is based on a rate equation of the growth and recombination of the defects at constant dose rate dD/dt. Following this model, the induced loss is determined approximately by two terms: one depends only on the total dose, while the other is dose rate dependent and tends to saturation with increasing total dose. The dose rate dependent term is conveniently represented by the sum of two (or more) saturated exponential components with different relaxation times.

During irradiation with dD/dt = constant, the growth of induced loss is described by:

$$\text{Loss (dB)} = \Sigma_i \{(L_i (1-\exp(-t/T(\text{irr})_i)\} + L_n t \qquad (i=1,..n-1)$$

while the recovery is given by:

$$\text{Recovery (dB)} = \Sigma_j \{(R_j \exp(-t/T(\text{rec})_j)\} + R_m \qquad (j=1,..m-1)$$

The index (i) corresponds to a type of defect in the fibre material and to the corresponding parameters and time constants.

The irradiation fit coefficients $L_i$ (i=1,..n-1) are *dose rate* dependent:

$L_i = A_i T(irr)_i dD/dt$, where $A_i$ are the damage constants in units of dB/Mrad,

whereas $L_n$ depends only on the *accumulated dose*.

The irradiation and recovery time constants are not necessarily identical. The damage and recovery fit parameters are shown in table A1-II.

Table A1-II - Damage and recovery constants from fit (normalised @ fibre length = 100m)

| SM Fibre type | PSC/$F_2$ (type 1) | PSC/$F_2$ (type 2) | Ge doped |
|---|---|---|---|
| $A_1$ (dB/Mrad) | 0.91 | 0.82 | 16.9 |
| $T(irr)_1$ (hr) | 4. | 4. | 1.6 |
| $R_1$ (dB) | 1.0 | 0.82 | 0.13 |
| $T(rec)_1$ (hr) | 0.12 | 0.11 | 0.2 |
| $A_2$ (dB/Mrad) | 0.63 | 0.62 | 0.75 |
| $T(irr)_2$ (hr) | 52. | 48.6 | 18.5 |
| $R_2$ (dB) | 0.9 | 0.82 | 0.81 |
| $T(rec)_2$ (hr) | 1.3 | 1.1 | 3.4 |
| $A_3$ (dB/Mrad) | 0.14 | 0.27 | 0.09 |
| $T(irr)_3$ (hr) | ∞ | ∞ | ∞ |
| $R_3$ (dB) | 2.6 | 2.45 | 5.2 |
| $T(rec)_3$ (hr) | 17.1 | 15.7 | 160. |
| $A_4$ (dB/Mrad) | | | |
| $R_4$ (dB) | 9.3 | 7.8 | 5.7 |

The time constants of the rate dependent irradiation and recovery terms are relatively short. To predict the induced loss at the LHC, we assume an operating cycle of the machine consisting of six months of irradiation with dD/dt Å 500rad/hr followed by six months of recovery. The overall contribution of the rate dependent terms will then be very low, and the corresponding residual induced loss will be fully recovered. The induced attenuation due to the linear term, in the worst case in which it would not recover during the six months of shutdown, is shown in table A1-III:

Table A1-III - Estimate of the γ-ray induced attenuation at LHC

| SM Fibre type | Induced loss (dB/100m) (1 year) |
|---|---|
| PSC/$F_2$ (type 1) | 0.3 |
| PSC/$F_2$ (type 2) | 0.6 |
| Ge doped | 0.2 |

Other investigators have found an induced attenuation smaller by a factor Å 2 in similar types of PSC/$F_2$ fibres at low dose rates. A more accurate prediction can be obtained by using lower dose rates (and longer irradiation time) and by monitoring the recovery for a longer period.

**References/Publications**


[1] CERN/DRDC/93-35 Status Report on the RD23 Project "Optoelectronic Analogue Signal Transfer for LHC Detectors" (Birmingham, CERN, EPFL Lausanne, Imperial College, Lund, Oxford, RAL)

[2] Nucl. Instr. and Meth. A344 (1994) 199

[3] K. Webster et al., Nucl. Instr. and Meth. A340 (1994) 384

[4] Project CERN/Uni Bern (K. Borer, R. Klingerberg)

[5] G. Hall and G. Stefanini, CMS TN/94-137

[6] J. Dowell et al., back-up document for the ATLAS Technical Proposal (in preparation)

[7] M. Haben's and K. Webster's thesis; also internal report by R. Cingolani and M. Glick

[8] R. Halsall, S. Quinton et al, Specification of the readout module for the CMS tracker (RAL)

[9] M. Kyoto et al., Journ. Lightwave Technology 10 (1992) 289

[10] K. Gill, F. Vasey et al., report in preparation


**Main contributions to conferences**

Int. Conf. on Computing in High Energy Physics, Annecy (1992)

6th European Conference on Integrated Optics, Neuchatel (1993)

5th Topical Seminar on Exp. Apparatus for HEP and Astrophysics, S. Miniato (1993)

Conference on Lasers and Electro-Optics (CLEO '94)

2nd Int. Meeting on Front End Electronics for Tracking Detectors at Future High Luminosity Colliders, Perugia (1994)

6th Pisa Meeting on Advanced Detectors, Elba (1994)

27th Int. Conf. on High Energy Physics, Glasgow (1994)

**PhD Thesis**

M. Haben, "Applications of Optoelectronics in High Energy Physics", Univ. of Birmingham (1993)

K. Webster, ibid. (in preparation)

W. Langhans, CERN (under way)